

Conference Paper

# Simulation and Optimization of Control of Selected Phases of Gyroplane Flight

Wienaczyslaw Stalewski <sup>1\*</sup>

<sup>1</sup> Institute of Aviation, Al. Krakowska 110/114, Warszawa, Poland; wienaczyslaw.stalewski@ilot.edu.pl

\* Correspondence: wienaczyslaw.stalewski@ilot.edu.pl; Tel.: +48-888-146-748

**Abstract:** The optimization methods are increasingly used to solve challenging problems of aeronautical engineering. Typically, the optimization methods are utilized in design of aircraft airframe or its structure. The presented study is focused on an improvement of aircraft-flight-control procedures through the numerical optimization approach. The optimization problems concern selected phases of flight of light gyroplane - a rotorcraft using an unpowered rotor in autorotation to develop lift and an engine-powered propeller to provide thrust. An original methodology of computational simulation of rotorcraft flight was developed and implemented. In this approach the aircraft-motion equations are solved step-by-step, simultaneously with the solution of the Unsteady Reynolds-Averaged Navier-Stokes equations, which is conducted to assess aerodynamic forces acting on the aircraft. As a numerical optimization method, the BFGS algorithm was adapted. The developed methodology was applied to optimize the flight-control procedures in selected stages of gyroplane flight in direct proximity of the ground, where properly conducted control of the aircraft is critical to ensure flight safety and performance. The results of conducted computational optimizations proved qualitative correctness of the developed methodology. The research results can be helpful in design of easy-to-control gyroplanes and also in the training of pilots of this type of rotorcraft.

**Keywords:** flight simulation; flight control; optimization; CFD; flight dynamics

## 1. Introduction

Optimization methods are widely considered to be a very effective tool that can significantly improve the performance and exploitation properties of contemporarily designed and constructed aircraft. Typically, the optimization methods are utilized in design of aircraft airframe or its structure that may be optimized simultaneously using a multi-disciplinary approach [1-3]. Fast development of both computational methods and computer hardware offers opportunities to expand the range of applications of optimization methods. As part of this trend, the application of modern computational methods to optimize aircraft-flight-control procedures is presented in this paper. The developed methodology for optimization of flight control procedures is discussed on the example of flight of a light gyroplane.

A gyroplane is an aerodyne equipped with unpowered main rotor and engine-powered propeller, generating a thrust force necessary to move the aircraft forward. During the gyroplane flight the air flowing around rotating blades of main rotor generates aerodynamic reaction whose vertical component balances the aircraft weight, while the aerodynamic moment is driving the main rotor that rotates in autorotation. However to induce the autorotation phenomenon, the rotor should be initially pre-rotated, which is usually done by the engine driving the propeller. Before the gyroplane loses contact with the ground, the drive of the rotor must be disconnected because this type of rotorcraft does not have any anti-torque devices.

Primary flight-control means of gyroplanes are:

- longitudinal and lateral tilting of the rotor shaft to ensure a pitch and roll control,
- deflections of the rudder to ensure a yaw control.

Gyroplanes may be optionally equipped with the following secondary flight controls:

- pre-rotator which drives the rotor to initiate its rotation,
- changeable collective pitch of rotor blades that may be used for torque reduction in pre-rotation and is necessary to conduct so called "jump takeoff".

The classic takeoff of a gyroplane is similar to typical takeoff of an airplane. The gyroplane, with pre-rotated main rotor, starts accelerated run along the runway. The rotor generates more and more thrust. When the thrust exceeds the weight of aircraft, the gyroplane takes off. Gyroplanes usually need short runway to conduct the classic takeoff and they mostly belong to STOL (Short Takeoff and Landing) type of aircraft.

In the case of so called "jump takeoff", the gyroplane takes off directly from the ground, without a run along the runway. To perform this maneuver, the rotor head design should allow changing an angle of blade collective pitch during the flight. After initial pre-rotation of the rotor, the drive is disconnected and simultaneously the higher angle of the blade collective pitch is established. The inertia-driven rotor generates high thrust, which makes that the gyroplane jumps upwards. The propeller starts driving the gyroplane in horizontal direction, which makes that the horizontal velocity starts growing and after some time the rotor starts rotating in autorotation, similarly as it is in a case of the classic takeoff.

All studies presented in this paper, have been conducted for a gyroplane presented in Figure 1. The gyroplane is equipped with a teetering main rotor, three-bladed tractor-type propeller, front landing gear and v-tail that also serves as a rear landing gear. Like in a case of most gyroplanes, the main rotor of the presented gyroplane is characterized by a simple design. It is two-bladed, teetering rotor. Its blades have a rectangular planform, uniform spanwise distribution of airfoil and are not twisted. To enhance the controllability of the gyroplane its rotor-head design enables to control the collective pitch of rotor blades.

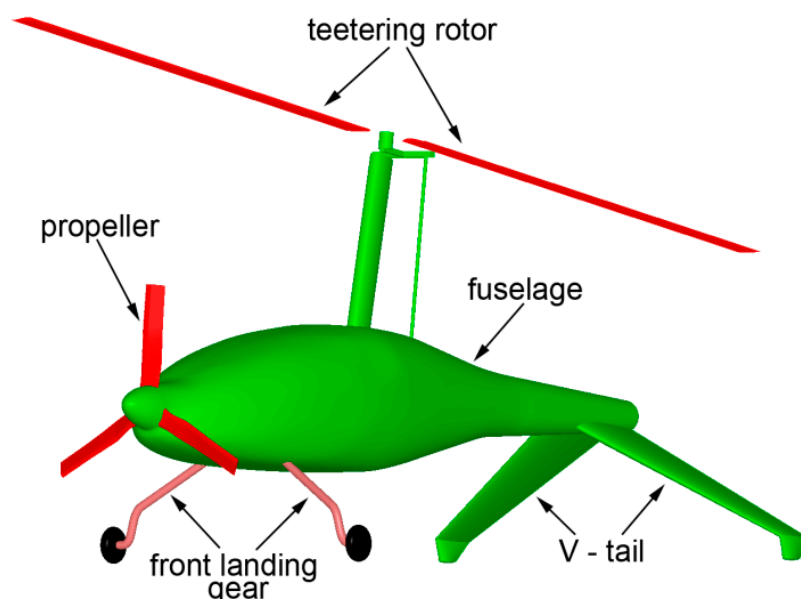


**Figure 1.** Model of the gyroplane being a subject of the research discussed in the paper.

An effective and safe takeoff of the gyroplane requires accurate and rapid deflections of flight-control devices. This especially concerns the control of the rotor-pitch angle that has to be changed in time optimally so as to enhance the autorotation effect as much as possible. Additionally, during the jump takeoff, the dynamic changes of the rotor-pitch angle have to be synchronized optimally with dynamic changes of the collective pitch of the rotor blades.

The main idea of the presented research was to search for possibly optimal procedures of control of the gyroplane flight through application of a numerical-optimization methodology. To realize this idea, the following three main goals of the research undertaken were established:

1. To develop a computational methodology of simulation of a gyroplane flight, especially directed towards high-fidelity simulations of a takeoff and ascent flight of the rotorcraft,
2. To develop a numerical-optimization methodology that would be applicable for the solving of problems concerning the optimization of rotorcraft-flight-control procedures,
3. To optimize flight-control procedures (i.e. functions describing time-variable settings of the flight-control devices) during the classic takeoff and jump takeoff of the gyroplane, so as to achieve measurable improvement in the aircraft performance in these flight states.

Numerical-optimization methods are wider and wider utilized in rotorcraft engineering. Most of them are directed towards optimization of the rotorcraft crucial components such as main rotors or tail rotors. Nowadays, such optimization problems are usually formulated in multidisciplinary form [4]. This includes more and more reliable methods in such areas as Computational Fluid Dynamics (CFD), Computational Structural Mechanics (CSM) or Flight Dynamics. On the other hand, attempts are made to automate the design process itself, by applying numerical optimization methods. The CFD methods have reached sufficient maturity to compute very accurately helicopter rotor aerodynamic performance. The current CFD codes efficiency enables potentially to use them in automatic optimization chains. Such optimization strategies involving URANS (Unsteady Reynolds-Averaged Navier-Stokes) solvers have been applied in aeronautics on fixed wing configurations [5,6] or via adjoint formulation on aircraft configurations [7,8] and have demonstrated their efficiency to be successfully integrated in design cycles. Alternative approaches are based on stochastic-optimization methods (e.g. Genetic Algorithm). Among others, such approach was applied in [3] for optimization of helicopter fuselage (with simulation of main and tail rotor influence) as well as in [1,2] for multidisciplinary optimization of aircraft wings. To cope with extreme complexity of coupling of advanced methods of CFD and numerical-optimization, some authors utilize surrogate models of physical phenomena, as presented in [9,10]. In [11] authors describe an optimization strategy for helicopter rotor blades shape, based on the coupling of an optimization gradient method with a 3D Navier-Stokes solver.

Advanced numerical optimization methods coupled with Navier-Stokes solvers, are actually used mostly for an optimization of aircraft external shapes (aerodynamic design) or its structure. In the case of optimization of the rotorcraft flight control procedures, simplified computational models of aircraft aerodynamics are usually used. In particular, it concerns advanced computational tools dedicated for flight-control optimization. Such tools utilize usually simple models of rotorcraft aerodynamics. The aerodynamic effects generated by crucial components of rotorcraft, such as main rotor or tail rotor, are usually modelled using the Lifting-Line Theory or even are based on databases of global aerodynamic characteristics of these rotors. In a case of rotorcraft-flight-control design-and-optimization tool named CONDUIT, the details concerning the utilized both optimization methods and aerodynamic models are discussed thoroughly in references [12,13].

In comparison to previously used computational tools supporting the design and optimization of rotorcraft flight control, the approach discussed in this paper is not directly geared to industrial applicability but rather to explore new solutions that could in future be applied in the practice of designing of flight-control systems. The proposed solution distinguishes itself from most of currently utilized approaches by the following assumptions:

- The rotorcraft-flight-control optimization is based on advanced, gradient-based optimization methods coupled with advanced CFD methods used directly during the rotorcraft-flight simulation for the current determination of aerodynamic loads acting on the aircraft.
- The developed methodology is applied to optimize the gyroplane-flight-control procedures (while most of the applications cited in the literature are focused on the optimization of helicopter-flight control).

## 2. Research Methodology

The general scheme of the developed methodology of rotorcraft-flight simulation is presented in Figure 2. The flight-simulation procedure is embedded in the URANS (Unsteady Reynolds

Averaged Navier Stokes) solver ANSYS FLUENT [14]. Flow effects caused by rotating lifting surfaces are modelled by application of the developed UDF (User Defined Function) module Virtual Blade Model (VBM) [3] that is compiled and linked with the essential code of the ANSYS FLUENT software. In the VBM approach, real rotors are replaced by volume discs influencing the flow field similarly as rotating blades. Time-averaged aerodynamic effects of rotating lifting surfaces are modelled by means of artificial momentum source terms placed inside the volume-disc zones placed in regions of activity of real rotors. Such zones, replacing the real rotor and propeller in investigated gyroplane, are shown in Figure 3. The momentum rates, injected from these zones into the fluid, are evaluated based on the Blade Element Theory, associating local flow parameters in rotor-disc zones with aerodynamic characteristics of blade airfoils. Data bases of these characteristics (in general: lift and drag coefficients as functions of angle of attack, for several sets of Mach and Reynolds numbers, similar to those that are expected on the real rotor blades) should be prepared before starting the flight simulation. The original VBM code was significantly modified and expanded by the author of this paper. Beside the essential modules ANSYS FLUENT and VBM, the methodology presented in Figure 2 utilizes two additional modules. The module FLIGHT-DYNAMIC gathers information of all momentary loads acting on the rotorcraft and solves 6 degree-of-freedom equations of rotorcraft motion. The module KINEMATICS is responsible for modelling of effects of motion and changes of rotorcraft geometry, which is realized through redefinition of boundary conditions for the ANSYS FLUENT solver and through deformations of computational mesh. The computational model of the gyroplane, shown in Figure 3, was developed so as to enable simulation of flight in proximity of the ground and tilting of the rotor. These motions are realized through appropriate deformations of computational mesh which is done with the use of the Dynamic Mesh technique, implemented in ANSYS FLUENT solver. Examples of such deformations of computational mesh are presented in Figure 4. Additionally, the developed model enables deflecting the gyroplane control surfaces (option not used in the presented study) which is realized through application of Sliding-Mesh and Non-Conformal-Interface techniques implemented in ANSYS FLUENT.

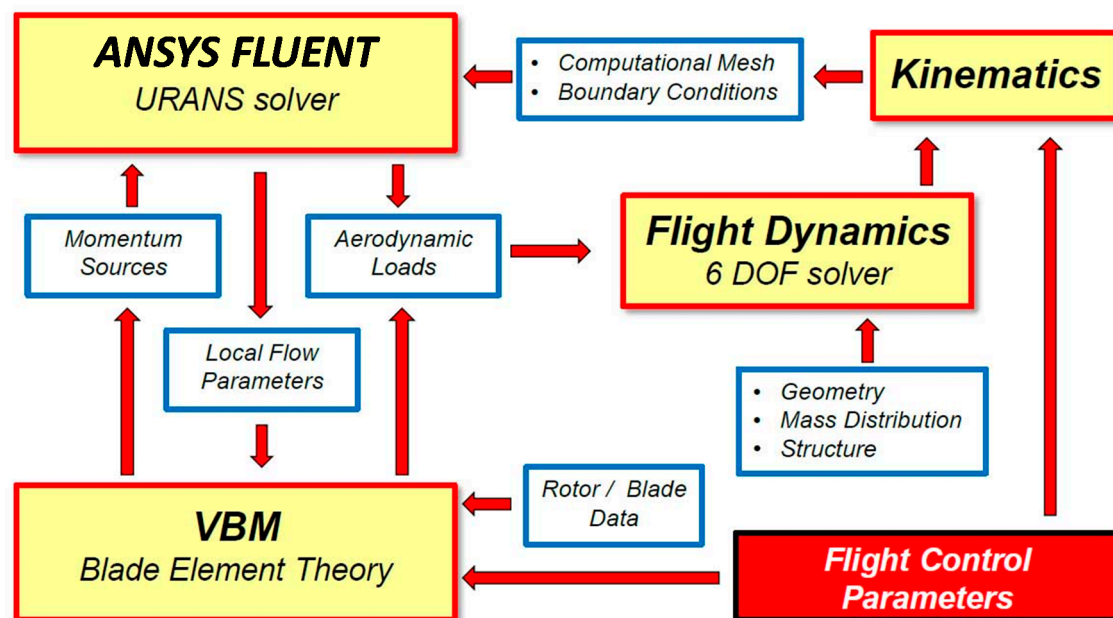


**Figure 2.** General scheme of the developed methodology of rotorcraft-flight simulation.

The described complex model of the gyroplane flight was used in optimization studies on flight-control procedures during the gyroplane takeoff. Though the developed methodology enables to solve 6-degree-of-freedom rotorcraft flight dynamics, the presented in the paper simulations were conducted taking into account only 3 degree-of-freedom system, limited to force-balance equations, while the moment-balance equations were omitted.



The method of computational simulation of gyroplane flight, has been applied in optimization studies on flight-control procedures. In these studies, functions describing changes in time of main gyroplane-flight-control means (i.e.: tilt of the main-rotor shaft and collective pitch of rotor blades) have been parameterized. They were uniquely defined by sets of few unknown real numbers - the design parameters. The objective function, considered as a function of unknown design parameters, was defined in presented examples as an altitude which would be achieved by the gyroplane, after reaching the assumed distance from the takeoff point. The optimization problem consisted in searching for the set of the design parameters that would maximize the objective function.

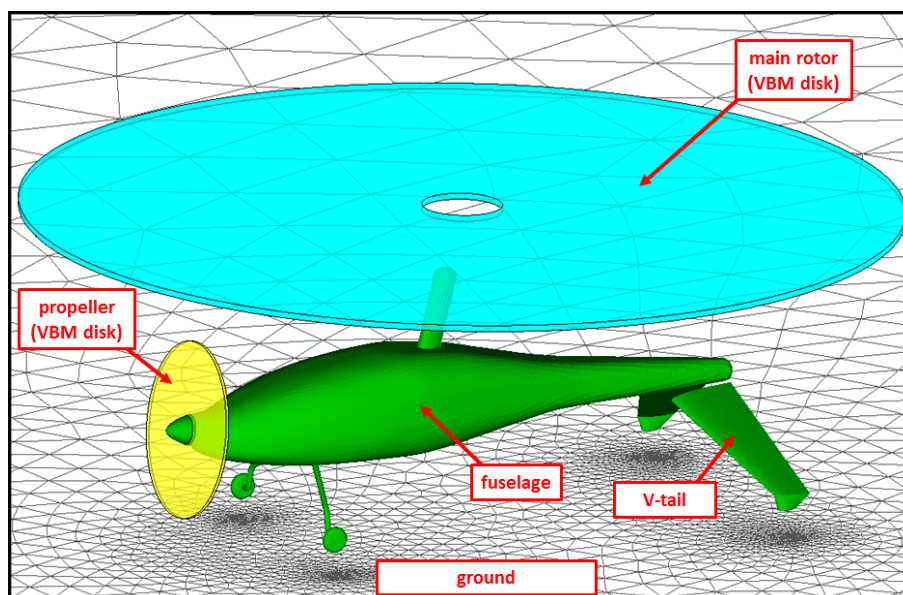


**Figure 3.** Computational model of the gyroplane flying in proximity of the ground.

To solve the defined above optimization problem, the appropriately adapted BFGS Algorithm [5] has been applied. The method BFGS, named after C.G. Broyden, R. Fletcher, D. Goldfarb and D. Shanno, belongs to quasi-Newton methods - a class of hill-climbing optimization techniques that seek a stationary point of a given objective function (preferably twice continuously differentiable). Gradient-based methods utilize a necessary condition for optimality, saying that at optimum point the gradient of objective function is a zero vector. Usually such methods do not guarantee the convergence to the exact optimum, unless the objective function has a quadratic Taylor expansion near an optimum. However, BFGS Algorithm has proven to have good performance even in such case when the objective functions were not smooth.

In quasi-Newton methods, including the BFGS Algorithm, the Hessian matrix of second derivatives does not need to be evaluated directly. Instead, the Hessian matrix is approximated using updates specified by gradient evaluations or approximate gradient evaluations. The latter approach has been applied in the presented optimization studies.

Like in all cases of gradient-based methods, the optimal solution has been searched for, in sequential iterative steps. In each step, the components of the gradient vector (partial derivatives of the objective function with respect to the unknown design parameters) were evaluated by means of one-sided finite-difference approximation. In the presented approach, this required performing at least  $N+1$  simulations of the gyroplane flight, where  $N$  was the number of the independent variables (design parameters). In addition, solving the typical for the BFGS method the auxiliary one-dimensional problem of finding the optimal movement in the newfound search direction, several additional simulations of gyroplane flight was conducted at each sequential step of the optimization process.

It should be mentioned, that the BFGS method has been developed also in a variant with simple box constraints [16] and usually such variant of the method has been applied in the presented optimization studies.

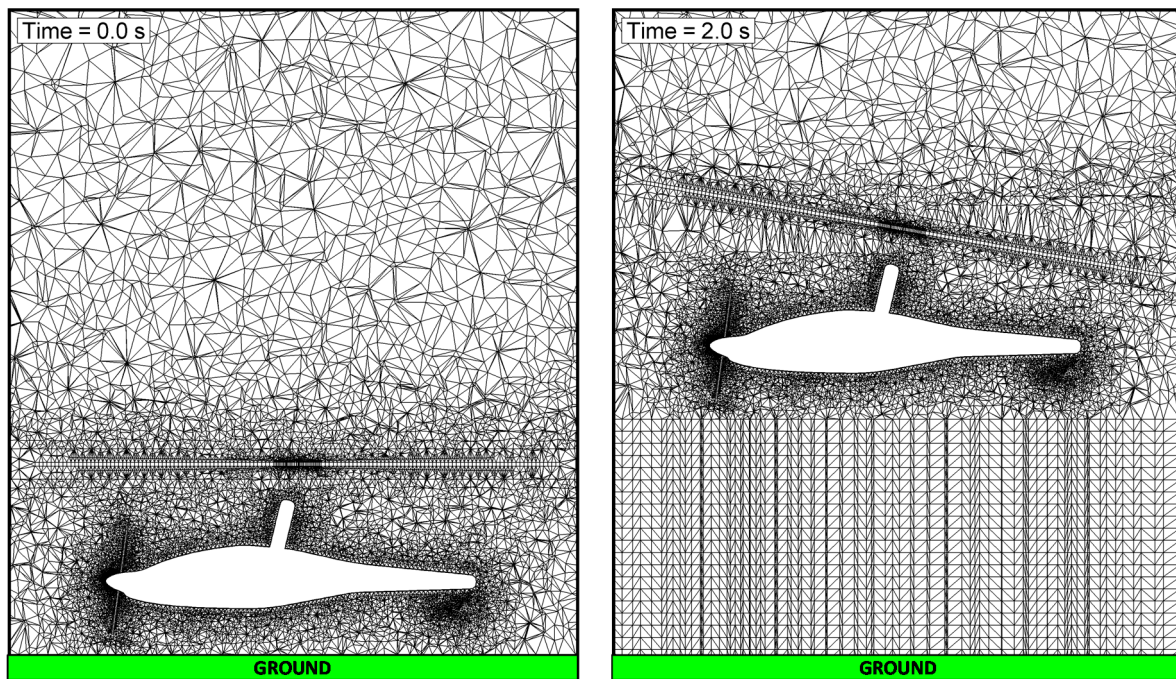


**Figure 4.** Cross-section of computational mesh around the gyroplane in two different stages of flight  
Left side: a ground pre-rotation, right side: a forward flight few meters above the ground.

### 3. Optimization of Gyroplane-Takeoff-Control Procedures

The presented below two examples of conducted numerical optimizations of gyroplane-flight-control procedures concern the described above two types of takeoff of the gyroplane: classic takeoff and jump takeoff. In both cases, the optimization process aimed at maximization of the altitude reached by the gyroplane after traveling certain distance from the takeoff place. The both optimizations were conducted for the same assumed general flight conditions:

- total mass of the gyroplane: 600 kg,
- maximum thrust of the propeller: 2943 N.

#### 3.1. Classic Takeoff of the Gyroplane

The optimization of classic-takeoff-control procedure has been conducted in respect to time-variable pitch angle of main rotor ( $\varphi_R$ ), which was considered as the only flight control parameter. The angle of collective pitch of rotor blades ( $\theta_0$ ), unchangeable during the flight, has been assumed as additional unknown parameter. Based on these assumptions, the flight control procedure during the classic takeoff has been defined by graphs presented in Figure 5, where:

- function  $\varphi_R(t)$  is uniquely defined by unknown parameters  $D_1$  and  $F_1$ ,
- constant function  $\theta_0(t) = \text{const.}$  is uniquely defined by unknown parameter  $F_2$ .

In this case, the optimization problem consisted in determination of optimal values of unknown parameters  $D_1$ ,  $F_1$  and  $F_2$ . The optimization aimed at maximization of the altitude ( $H$ ) reached by the gyroplane after traveling the distance  $X=200$  m from the takeoff place, which is explained in Figure 6. The optimization problem was formulated in mathematical terms as a search for the set of the design parameters  $D_1$ ,  $F_1$  and  $F_2$  maximizing the following function  $\Phi$ :

$$\Phi(D_1, F_1, F_2) = H(X=200\text{m}), \quad (1)$$

taking into account the following constraints:

$$D_1 > 1, \quad (2)$$

$$F_2 \leq \theta_{0\max}, \quad (3)$$

$$|F_1/D_1| \leq \lambda_1, \quad (4)$$

$$F_1 \leq \varphi_{R\max}, \quad (5)$$

where:  $\lambda_1$  - limit of angular speed of change of  $\varphi_R$ ,  $\varphi_{R\max}$  - maximum of rotor pitch and  $\theta_{0\max}$  - maximum of blade collective pitch.

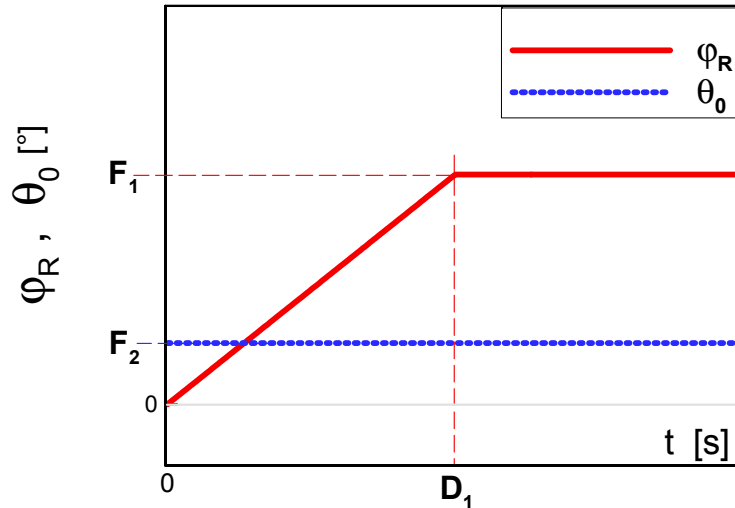


**Figure 5.** Parametric model of the gyroplane-flight-control procedure utilized in the optimization of classic takeoff of the gyroplane.

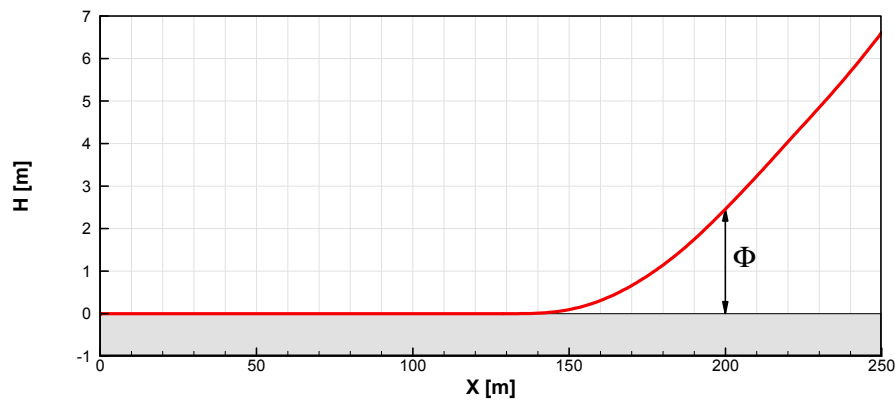


**Figure 6.** Definition of the objective ( $\Phi$ ) for the optimization of classic-takeoff-control strategy.

The optimization problem has been solved iteratively using the BFGS Algorithm, discussed in section 2. The assumed initial classic-takeoff-control procedure is presented by the graphs shown on the left side in Figure 8. In the sequential steps of the optimization process, this procedure has been improved from the point of view of maximizing the objective  $\Phi$  (1). In each iterative step, the partial derivatives of the objective function  $\Phi$  with respect to the unknown design parameters had to be approximated due to requirements of the BFGS Algorithm. These derivatives were evaluated by means of the one-sided finite-difference approximation. This required performing at least  $N+1$  simulations of the classic takeoff of the gyroplane, where  $N=3$  was the number of the independent variables of the objective (1). In addition, solving the auxiliary one-dimensional problem of finding the optimal movement in the newfound search direction, 8 additional gyroplane-classic-takeoff simulations were conducted at each optimization step.

In the presented optimization process, 4 iterative steps of the BFGS method have been conducted. Changes of the objective function  $\Phi$  in the sequential steps are shown in Figure 7. The presented results show that at a distance of 200 meters, the gyroplane controlled by the

optimized procedure reached about 5 meters higher altitude than the baseline. The significantly improved final flight-control procedure is compared with the initial procedure in Figure 8.

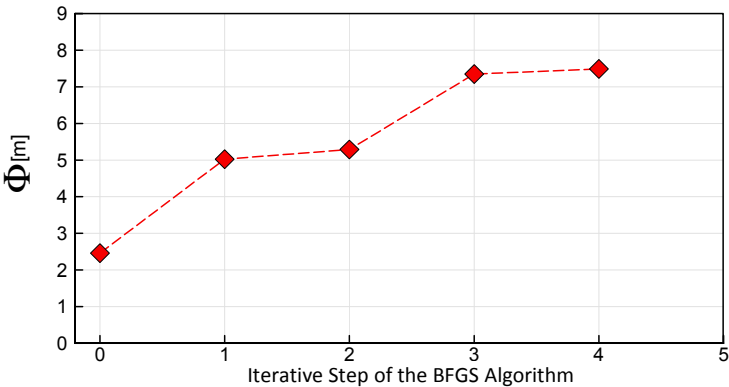


**Figure 7.** Values of the maximized objective  $\Phi$  in sequential iterative steps of the process of optimization of the classic-takeoff-control procedure of the gyroplane.

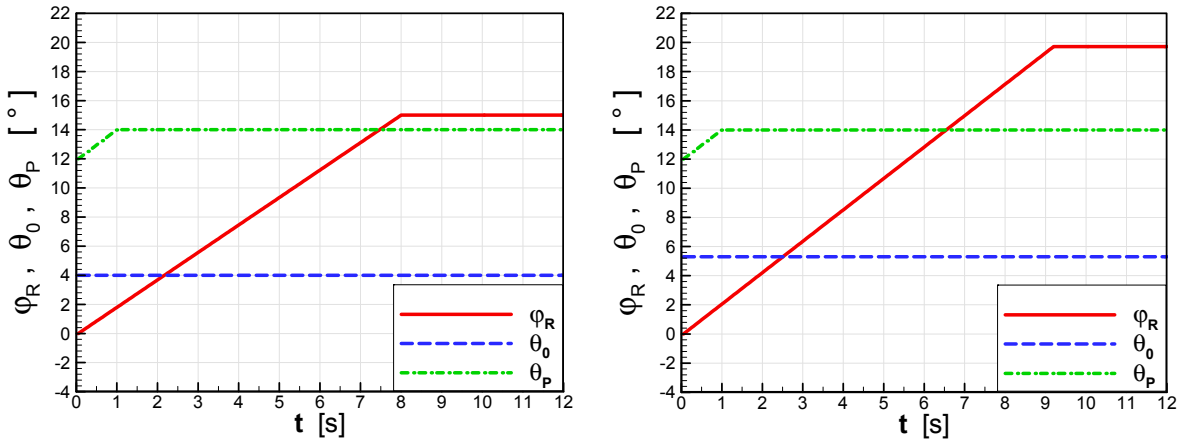


**Figure 8.** Comparison of the initial (left graph) and optimized (right graph) classic-takeoff-control procedures. The pitch angle of main rotor ( $\phi_R$ ), collective pitch of rotor blades ( $\theta_0$ ) and collective pitch of propeller blades ( $\theta_P$ ) as functions of time ( $t$ ).

The final solution of the optimization over the initial procedure differs in the blade collective pitch greater by  $1.3^\circ$ , the rotor pitch angle greater by  $4.7^\circ$  and angular speed of change of rotor pitch greater by 14.3%. Figure 9 compares gyroplane-flight trajectories during the classic takeoff for two gyroplane-flight-control strategies: initial and optimized. Compared to the initial flight-control procedure, the aircraft trajectory corresponding to the optimized procedure shows a shorter run of the aircraft on the runway and faster climb, at least during the arrival to the assumed altitude-control point, localized 200 m from the starting point. As shown in Figure 10, after some time ( $t > 20$  sec) the flight altitude of the gyroplane controlled according to the initial procedure begins to exceed that achieved by the gyroplane controlled by the optimized procedure. However, at the distance 200 m, the gyroplane controlled by the optimized procedure reached the flight altitude higher by approximately 5 meters, which confirms that the optimization process has finished successfully.

Figures 11 – 13 present snapshots of flow field (visualized through velocity magnitude contours) around the gyroplane, taken during the classic-takeoff simulation at time moments  $t=0, 10, 17.5$  sec (time elapsed from the beginning of the aircraft run on a runway), for two compared flight-control strategies : initial and optimized.



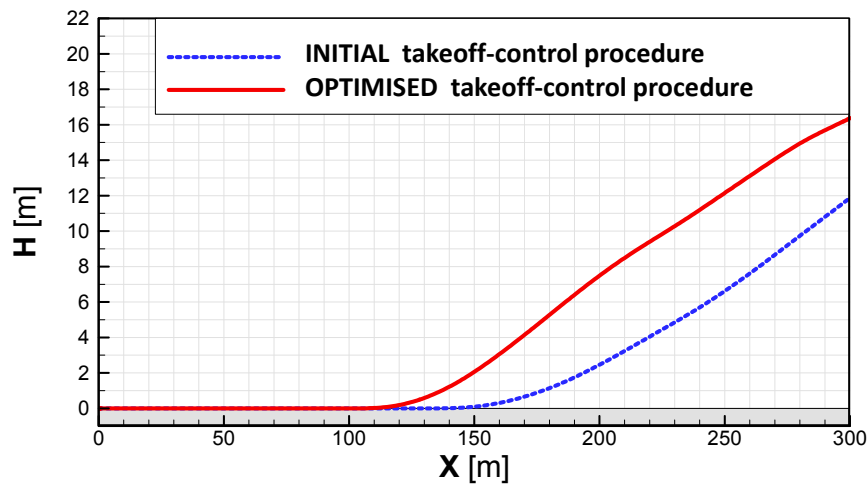


**Figure 9.** Aircraft trajectories obtained for the initial and optimized procedures of flight control during the classic takeoff of the gyroplane.

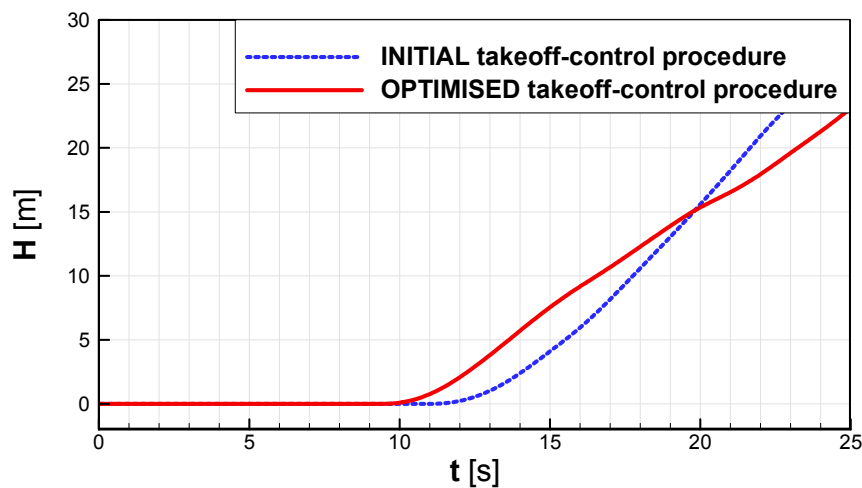


**Figure 10.** Aircraft flight altitude (H) vs time (t) during the classic takeoff, for the initial and optimized procedures of gyroplane-flight control.

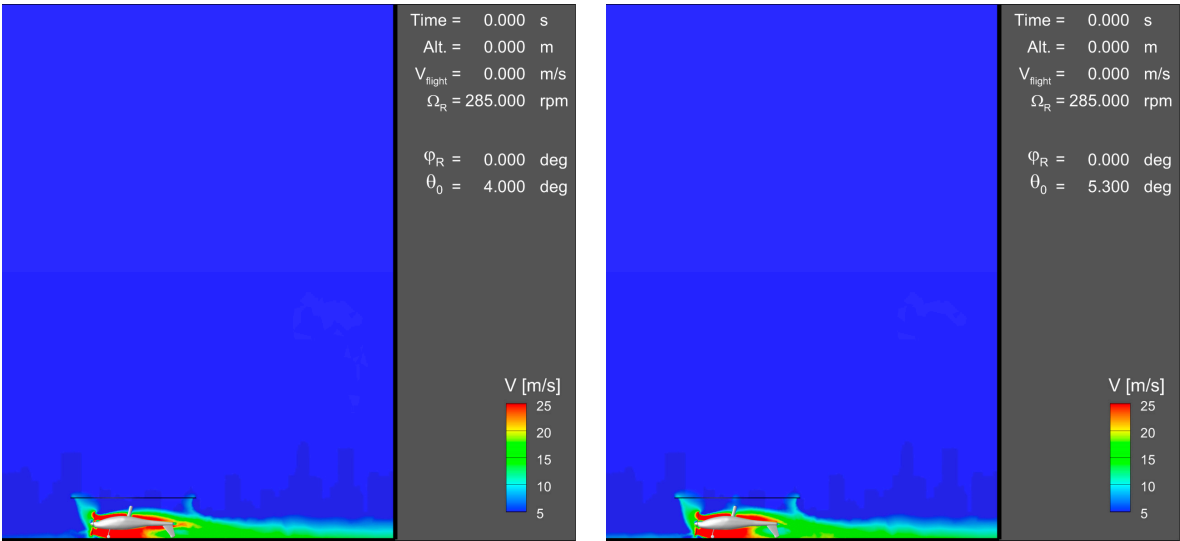


**Figure 11.** Comparison of velocity-magnitude contours around the gyroplane during the classic takeoff, for two configurations related to initial (left picture) and optimized (right picture) flight-control procedures. The initial time ( $t=0$  sec.) of the aircraft run on a runway.

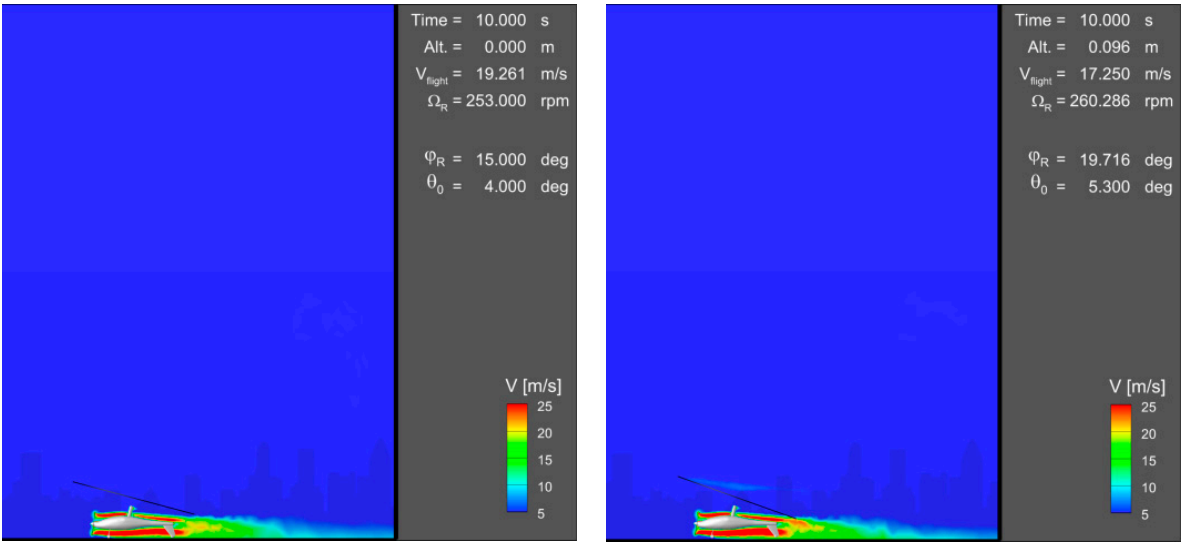


**Figure 12.** Comparison of velocity-magnitude contours around the gyroplane during the classic takeoff, for two configurations related to initial (left picture) and optimized (right picture) flight-control procedures. Time elapsed from the beginning of the aircraft run:  $t=10$  sec.

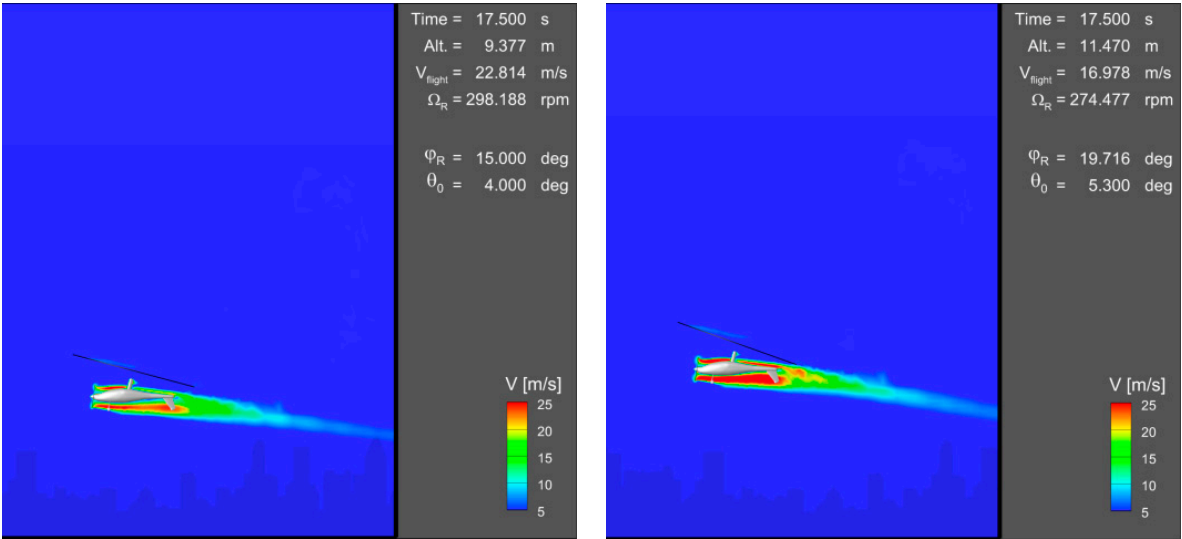


**Figure 13.** Comparison of velocity-magnitude contours around the gyroplane during the classic takeoff, for two configurations related to initial (left picture) and optimized (right picture) flight-control procedures. Time elapsed from the beginning of the aircraft run:  $t=17.5$  sec.

### 3.2. Jump Takeoff of the Gyroplane

Improvement of gyroplane-flight-control strategy during the jump takeoff was conducted based on numerical optimization approach described in section 2. In this case, the optimization was conducted in respect to the time-variable pitch angle of main rotor ( $\varphi_R$ ) and angle of collective pitch of rotor blades ( $\theta_0$ ). These two flight-control means were parameterized in a manner shown in Figure 14, where:

- function  $\varphi_R(t)$  is uniquely defined by unknown parameters:  $D_1$ ,  $D_2$  and  $F_1$ ,
- function  $\theta_0(t)$  is uniquely defined by unknown parameters:  $D_3$ ,  $D_4$ ,  $F_2$  and  $F_3$ .

The optimization problem consisted in determination of optimal values of unknown parameters  $D_1$ ,  $F_1$  and  $F_2$ . The optimization aimed at maximization of the altitude ( $H$ ) reached by the gyroplane after traveling the distance  $X=100$  m from the jump-takeoff place, which is explained in Figure 15. The optimization problem was formulated in mathematical terms as a search for the set of the design parameters:  $D_1$ ,  $D_2$ ,  $D_3$ ,  $D_4$ ,  $F_1$ ,  $F_2$  and  $F_3$ , maximizing the following function  $\Phi$ :

$$\Phi(D_1, D_2, D_3, D_4, F_1, F_2, F_3) = H(X=100m) \quad (6)$$

288 taking into account the following constraints:

$$D_1 \geq 0, D_2 \geq 1, D_3 \geq 0, D_4 \geq 1, \quad (7)$$

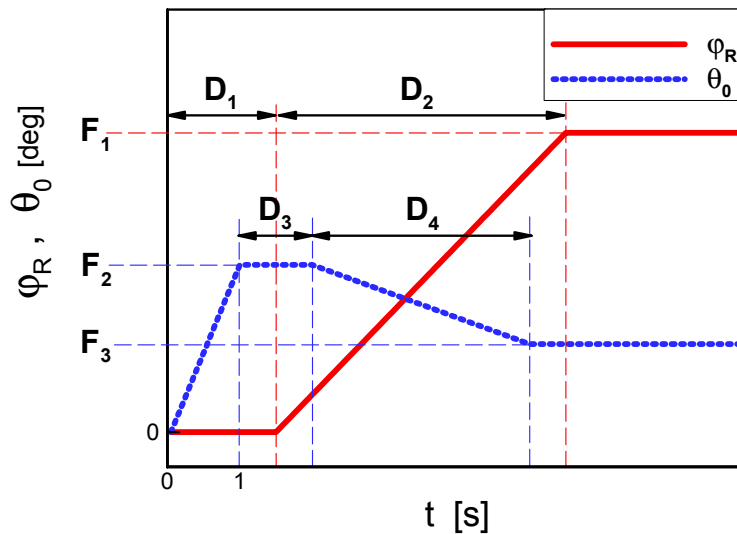
$$F_2 \leq \theta_{0\max}, \quad (8)$$

$$|F_1/D_2| \leq \lambda_1, \quad (9)$$

$$|(F_2-F_3)/D_4| \leq \lambda_2, \quad (10)$$

$$F_1 \leq \varphi_{R\max}, \quad (11)$$

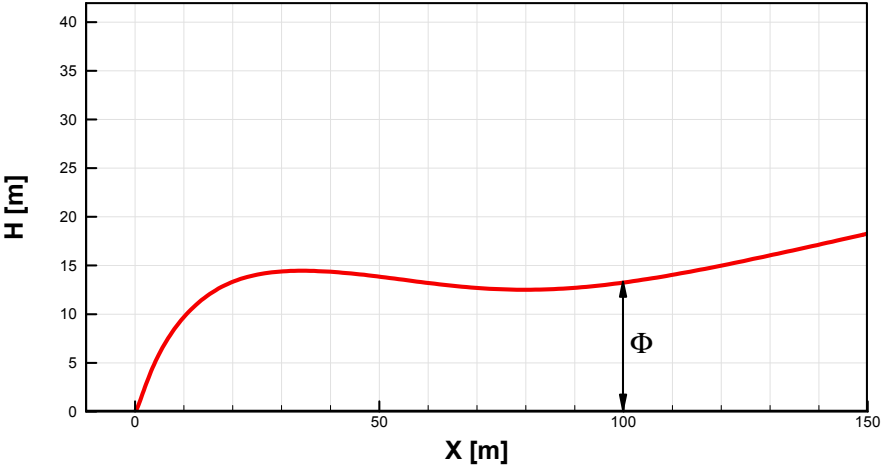
289 where:  $\lambda_1, \lambda_2$  - limits of angular speed of changes of  $\varphi_R$  and  $\theta_0$  respectively,  $\varphi_{R\max}$  – maximum of rotor  
 290 pitch and  $\theta_{0\max}$  maximum of blade collective pitch. The defined optimization problem has been  
 291 solved by application of the BFGS Algorithm. At every step of iterative process of the optimization,  
 292 the gradient of the objective function (6) was determined using the one-sided finite-difference  
 293 approximation. This needed to conduct at least  $N+1$  (where  $N=7$ ) independent simulations of  
 294 gyroplane jump takeoff for different sets of values of unknown design parameters  $D_1, D_2, D_3, D_4, F_1,$   
 295  $F_2$  and  $F_3$ . In addition, solving the auxiliary one-dimensional problem of finding the optimal  
 296 movement in the newfound search direction, 8 additional gyroplane-jump-takeoff simulations were  
 297 performed at each optimization step.



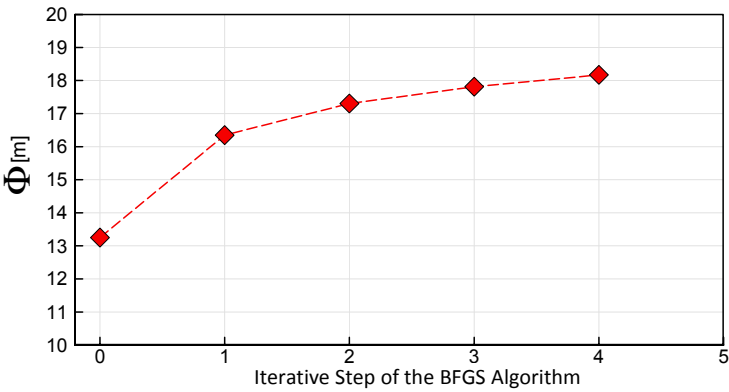
298 **Figure 14.** Parametric model of the gyroplane-flight-control procedure utilized in the optimization  
 299 of jump takeoff of the gyroplane.

300 The initial flight-control strategy was assumed in the form presented on a left side of Figure 17.  
 301 The optimization process consisted in gradual improvement of this strategy, so as to increase as  
 302 much as possible the objective (6). In the presented optimization process, 4 iterative steps of the  
 303 BFGS Algorithm have been conducted. Changes of the objective  $\Phi$  (6) in the sequential steps are  
 304 presented in Figure 16. The final solution of the optimization is presented on the right side  
 305 in Figure 17. The presented results show that the optimized flight-control strategy is characterized  
 306 by nearly the same values of parameters  $F_2$  and  $F_3$ . This means that these two parameters might be  
 307 replaced by only one in the assumed parametric model of flight-control strategy (shown in Figure  
 308 14) and the phase of decreasing of the rotor pitch, assumed in this model might be omitted. Figure 18  
 309 compares gyroplane-flight trajectories during the jump takeoff for two gyroplane-flight-control  
 310 strategies: initial and optimized. It may be concluded that optimized trajectory is growing  
 311 monotonically while the initial trajectory has a local minimum. Additionally, for the optimized  
 312 flight-control strategy the objective function (6) is higher by approximately 5 m than for the initial

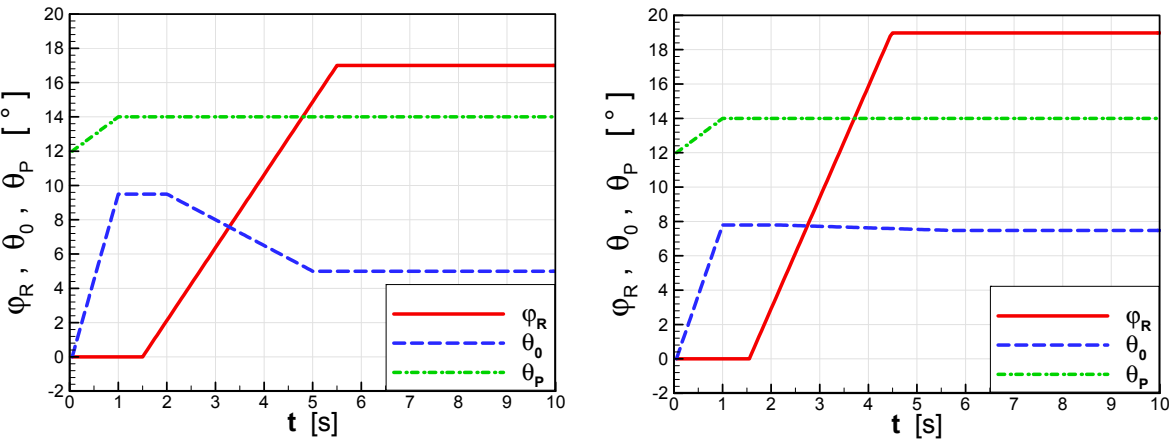
313 strategy. Similar advantages of the optimized flight-control procedure are presented in Figure 19,  
314 where dependencies of flight altitude (H) versus time (t) are compared, for the initial and optimized  
315 procedures. Figures 20 - 22 present snapshots of flow field (visualized through velocity magnitude  
316 contours) around the gyroplane taken during the jump-takeoff simulation at time moments  $t=0.5$ ,  
317 1.5, 10 sec (time elapsed from the beginning of the jump takeoff), for two compared flight-control  
318 strategies: initial and optimized.



319 **Figure 15.** Definition of the objective ( $\Phi$ ) for the optimization of jump-takeoff-control strategy.

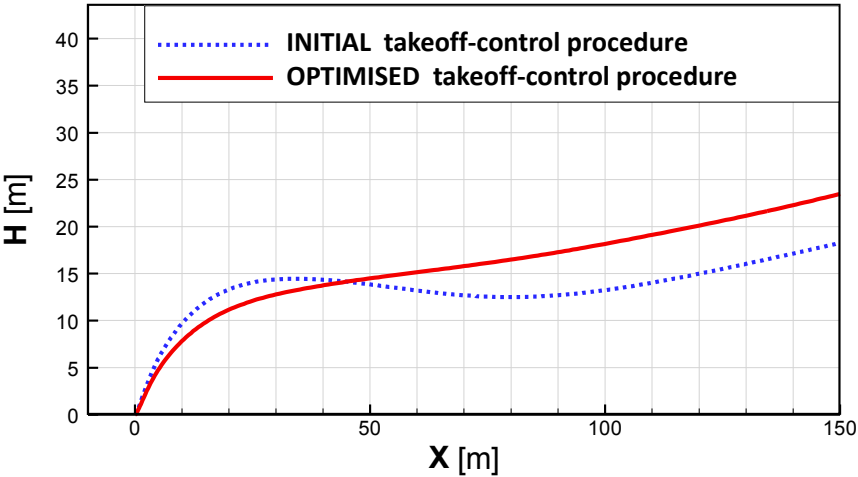


320 **Figure 16.** Values of the maximized objective  $\Phi$  in sequential iterative steps of the process of  
321 optimization of the jump-takeoff-control procedure of the gyroplane.

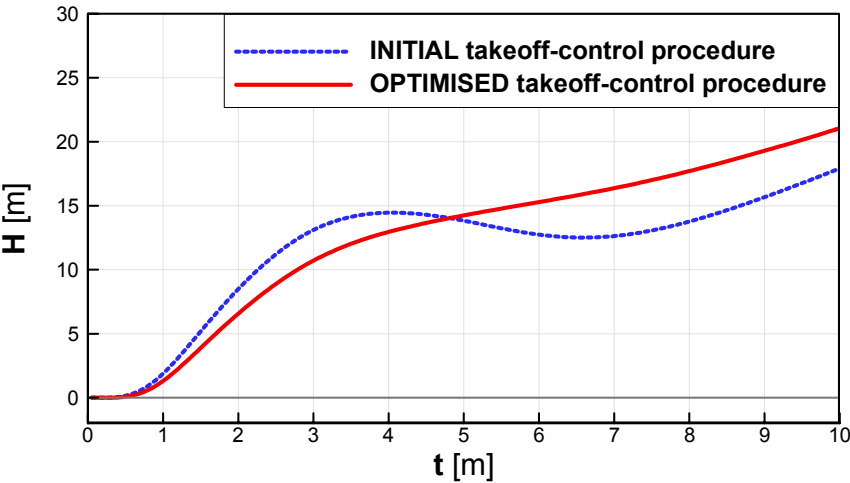


322 **Figure 17.** Comparison of the initial (left graph) and optimized (right graph) jump-takeoff-control  
323 procedures. The pitch angle of main rotor ( $\varphi_R$ ), collective pitch of rotor blades ( $\theta_0$ ) and collective pitch  
324 of propeller blades ( $\theta_P$ ) as functions of time (t).

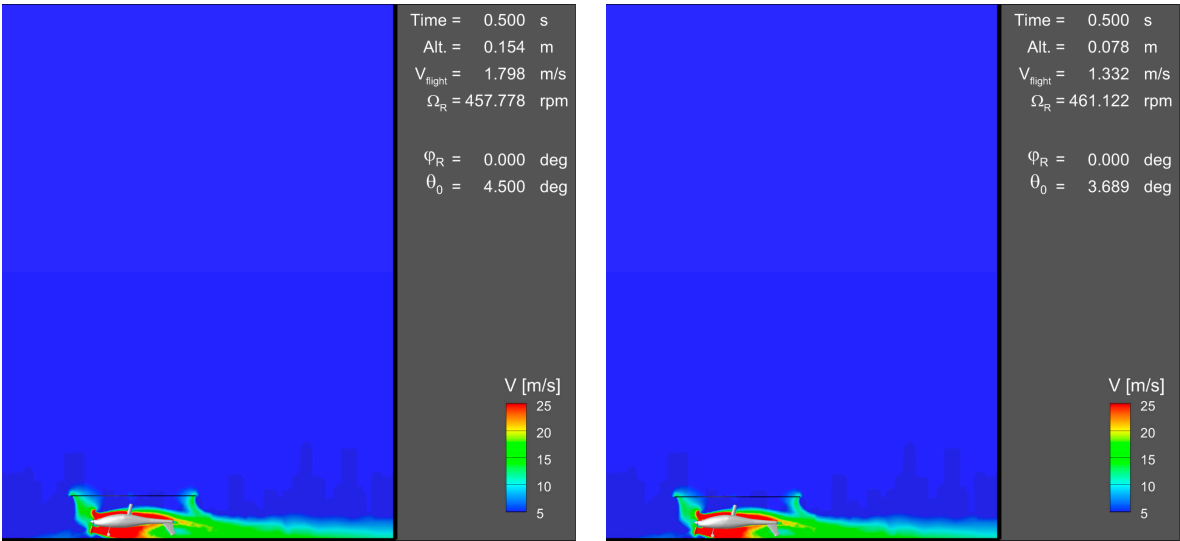




325 **Figure 18.** Aircraft trajectories obtained for the initial and optimized procedures of flight control  
326 during the jump takeoff of the gyroplane.



327 **Figure 19.** Aircraft flight altitude (H) vs time (t) during the jump takeoff, for the initial and optimized  
328 procedures of gyroplane-flight control.



329 **Figure 20.** Comparison of velocity-magnitude contours around the gyroplane during the jump  
330 takeoff, for two configurations related to initial (left picture) and optimized (right picture)  
331 flight-control procedures. The initial time moment ( $t=0.5$  sec) of the jump takeoff.

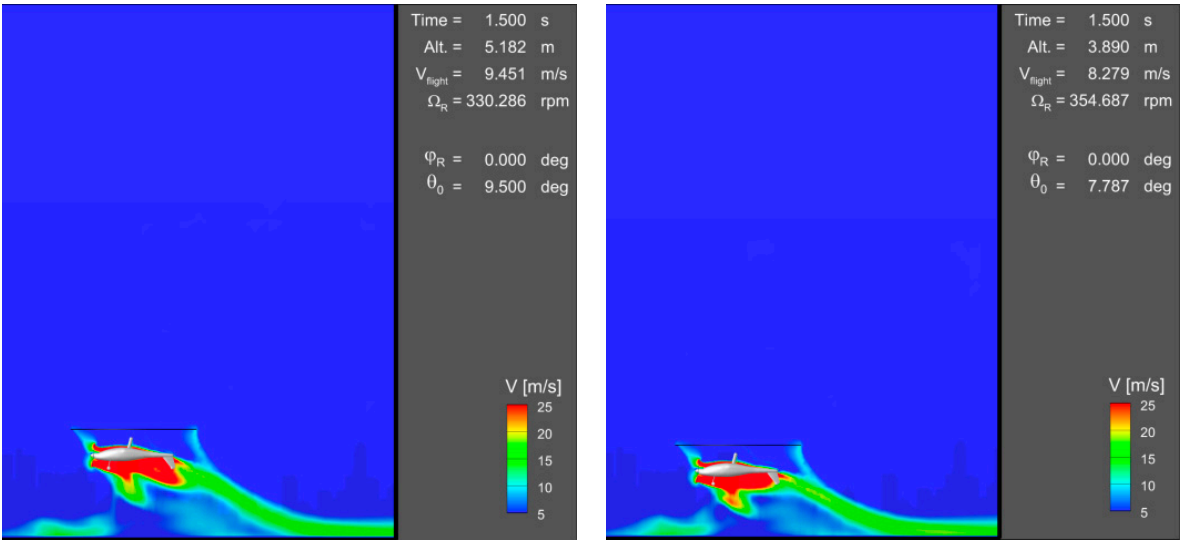


**Figure 21.** Comparison of velocity-magnitude contours around the gyroplane during the jump takeoff, for two configurations related to initial (left picture) and optimized (right picture) flight-control procedures. Time elapsed from the beginning of the jump takeoff:  $t=1.5$  sec.

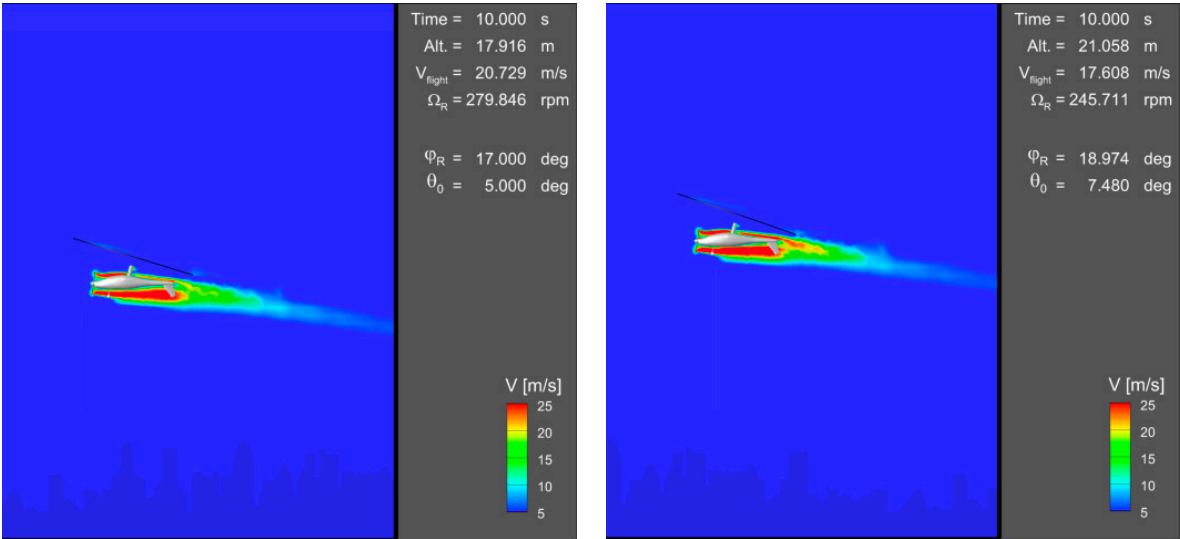


**Figure 22.** Comparison of velocity-magnitude contours around the gyroplane during the jump takeoff, for two configurations related to initial (left picture) and optimized (right picture) flight-control procedures. Time elapsed from the beginning of the jump takeoff:  $t=10$  sec.

#### 4. Discussion

A methodology of computational simulation of gyroplane flight has been developed. The methodology was applied to simulate classic takeoff of gyroplane and so called "jump takeoff" - the maneuver in which the gyroplane takes off similarly to a helicopter, without the accelerating run along a runway. For these two specific flight conditions, a numerical optimization of flight-control procedures has been conducted, using the gradient-based method - BFGS Algorithm. Within this process, the assumed design parameters described the time-variable settings of gyroplane-flight-control means: tilt of main-rotor shaft and collective pitch of rotor blades. The optimization aimed at determination of flight-control procedures optimal from point of view of possibly the highest altitude, reached by the gyroplane at an assumed distance, during both the classic takeoff and the jump takeoff.

In the both discussed cases of optimization, the gyroplane controlled according to the optimized strategy, reached by approximately 5 meters higher altitude than gyroplane manned according to the initial flight-control procedure. The presented exemplary computational

optimizations have proven qualitative correctness of the developed methodology. So far the obtained results have not been validated experimentally. The main reason of that is that the gyroplane being a subject of the investigations has not yet started its flight tests. It is expected that in the case of another selection of design parameters or another definition of the objective function, the optimization methodology developed would also confirm its effectiveness and reliability.

The research results can be helpful in the process of design of easy-to-control gyroplanes and also in the training of pilots of this type of rotorcraft. However, the presented methodology, seems to have much wider potential of future applications. These possible applications may concern not only other gyroplanes or in general: rotorcrafts but also may be utilized for optimization flight-control procedures of any aircraft, e.g. taking off or landing airplane.

## References

1. Rokicki, J.; Stalewski, W.; Zoltak, J. Multi-Disciplinary Optimization of Forward-Swept Wing, In *Evolutionary and Deterministic Methods for Design, Optimization and Control with Applications to Industrial and Societal Problems (A Series Of Handbooks On Theory And Engineering Applications Of Computational)*, Burczynski, T., Périaux, J., Eds.; 2011; pp. 253-259.
2. Stalewski, W., Zoltak, J., Design of a turbulent wing for small aircraft using multidisciplinary optimization, *Archives of Mechanics*, Volume 66 (3), 2014; pp. 185-201.
3. Stalewski, W., Zoltak, J. Optimization of the Helicopter Fuselage with Simulation of Main and Tail Rotor Influence, *Proceedings of the 28th ICAS Congress of the International Council of the Aeronautical Sciences*, ICAS, Brisbane, Australia, 2012.
4. Chattopadhyay, A., McCarthy, T.R., A multidisciplinary optimization approach for vibration reduction in helicopter rotor blades, *Computers & Mathematics with Applications* 25(2), January 1993, pp. 59-72.
5. Choi, S., Potsdam, M., Lee, K., Iaccarino, G., and Alonso, J. J., Helicopter Rotor Design Using a Time-Spectral and Adjoint-Based Method, *Journal of Aircraft*, Vol. 51, (2), 2014, pp. 412-423.
6. Choi, S., Datta, A., and Alonso, J. J., Prediction of Helicopter Rotor Loads Using Time-Spectral Computational Fluid Dynamics and an Exact Fluid-Structure Interface, *Journal of the American Helicopter Society*, 56, 042001 (2011).
7. Imiela, M., High-Fidelity Optimization Framework for Helicopter Rotors, *Aerospace Science and Technology*, Vol. 23, (1), December, 2012, pp. 2-16.
8. Johnson, C., and Barakos, G., Optimizing Aspects of Rotor Blades in Forward Flight," *AIAA 2011-1194*, *Proceedings of the 49th AIAA Aerospace Sciences Meeting including the New Horizons Forum and Aerospace Exposition*, Orlando, FL, January, 2011.
9. Glaz, B., Friedmann, P. P., and Liu, L., Surrogate Based Optimization of Helicopter Rotor Blades for Vibration Reduction in Forward Flight, *Structural and Multidisciplinary Optimization*, Vol. 35, (4), June 2008, pp. 341-363.
10. Glaz, B., Friedmann, P. P., and Liu, L., Helicopter Vibration Reduction throughout the Entire Flight Envelope Using Surrogate-Based Optimization, *Journal of the American Helicopter Society*, 54, 2009.
11. Le Pape, A., Beaumier, P., (2005), Numerical optimization of helicopter rotor aerodynamic performance in hover, *Aerospace Science & Technology*. April, Vol. 9 Issue 3, pp. 191-201.
12. Tischler, M. B., Colbourne, J. D., Morel, M.R., Biezad D.J., Levine, W. S., Moldoveanu, V., CONDUIT—A New Multidisciplinary Integration Environment for Flight Control Development, *NASA Technical Memorandum 112203 USAATCOM Technical Report 97-A-009*, June 1997.
13. Tischler, M. B., Berger, T., Ivler, C. M., Mansur, M. H., Cheung, K. K., Soong, J. Y., *Practical Methods for Aircraft and Rotorcraft Flight Control Design: An Optimization-Based Approach*, published by American Institute of Aeronautics and Astronautics, April 1, 2017.
14. ANSYS FLUENT User's Guide. Release 15.0. Available online: <http://www.ansys.com>.
15. Nocedal, J., Wright, S.J. *Numerical Optimization*, Springer-Verlag, 2<sup>nd</sup> Ed., Berlin - New York, 2006.
16. Byrd, R. H., Lu, P., Nocedal, J., Zhu, C., A Limited Memory Algorithm for Bound Constrained Optimization", *SIAM Journal on Scientific Computing*, 16 (5), 1995, pp. 1190-1208.